Physicochem. Probl. Miner. Process. 48(2), 2012, 413−424

www.minproc.pwr.wroc.pl/journal/

Physicochemical Problems
of Mineral Processing

ISSN 1643-1049 (print)
ISSN 2084-4735 (online)

Received January 5, 2012; reviewed; accepted March 1, 2012

HEAT TREATMENT OF NATURAL DIATOMITE

Suzan S. IBRAHIM*, Ali Q. SELIM**

*Central Metallurgical R&D Institute CMRDI, P.O. Box 87, Helwan, Egypt, suzansibrahim@gmail.com
** Geology Dept., Faculty of Science, Beni Suif Univ., Egypt

Abstract. Heat treatment of an Egyptian natural diatomite was performed at different temperatures (600, 900, 1000, 1100, and 1200ºC). The samples were heated from room temperature 23±1ºC to the appointed temperature at a rate of 20^oC/ min, and kept at that temperature for 5 hour. The heat treated samples were examined by X-ray diffraction, scan-electro-microscopy, and other physical characters like sample color, texture, and weight reduction. Results showed that heat treatment of natural diatomite caused different forms of mineral modification and transformation to another mineral. At 1200ºC a new nano-metric silicate material was formed. These changes were mainly depending upon the treated temperature, diatomite genera, and the accompanied gangue minerals as well.

keywords: natural diatomite, heat treatment, porous structure

1. Introduction

Diatoms are belonging to the diploid eukaryotic unicellular algae (Bacillariophyta) with wide ranges of structures and shapes. Each of these has its own distinct shape and size (Sterrenburg et al., 2007). The outstanding feature of diatoms is their siliceous “shell” or frustule, which can be preserved for millions of years. In this manner, fossil deposits of microscopic diatom shells were built up as thick layers of “diatomaceous earth” or diatomite which could be extending over several miles (Sterrenburg et al., 2007).

Diatomite is formed by the closest packing of hydrous SiO_2 spheres and is classified as opal-A. Opaline minerals have been categorized into three general groups, including Opal-A, Opal-C, and Opal-CT, according to crystallinity and crystal structure (Jones and Segnit, 1971). Opal-A is predominantly amorphous. Opal-CT is semi-crystalline comprising of crystalline regions of cristobalite and tridymite, where opal-C is a well-ordered form of the silicate predominantly in the cristobalite form (Jones and Segnit, 1971). Diatomaceous silica, the amorphous silica with opal-A structure, exists in the form of frustule in the natural mineral assemblage of diatomite. Since the diatomaceous silica has properties such as high porosity with strong absorbability and excellent thermal resistance, diatomite has been widely used as filter aid, catalytic support, biological support, functional filler, and adsorbent, etc.

http://dx.doi.org/10.5277/ppmp120208

(Erdogan et al., 1996; Ibrahim and Selim, 2011; Li et al., 2003; Powers and Ibrahim, 2007; Vasconclos et al., 2000).

As is well known, the silica surface consists of siloxane bridges and different types of hydroxyl groups (i.e. silanols), which are key reactive sites for various surface reactions: wetting, dispersion in solutions, adsorption and surface modification (e.g. silylation) etc. (Ek et al., 2001; Takei et al., 1999). The distribution and evolution of different types of silanols and siloxanes largely depend on thermal treatment condition, as well as on ambient humidity and storage time (Bronnimann et al., 1988).

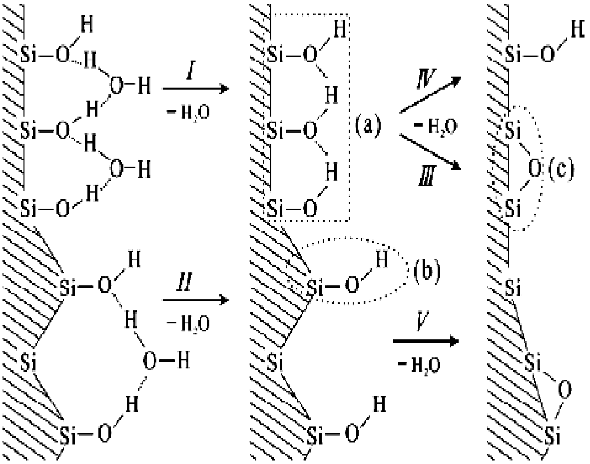

Fig. 1. The hydroxyl structure and the dehydration process of diatomaceous silica
(a) H-bonded silanols, (b) isolated silanols, (c) siloxane (Yuan et al., 2004)

At room temperature, both of the isolated and H-bonded silanols associate with the physically adsorbed water by hydrogen bond. After calcinations treatment, physically adsorbed water will be desorbed from the silanols, and the silanols will condense with the increase of temperature. Generally, the H-bonded silanols condense more easily than the isolated ones (Yuan et al., 2004). A model is proposed to elucidate the hydroxyl structure and the dehydration process of diatomite. At room temperature, both the isolated and H-bonded hydroxyl groups on the diatomite surface are H-bonded with physically adsorbed water. With the increase of temperature of 200 - 1000ºC, five dehydration processes are assumed, shown as scheme *I* to *IV* in Fig. 1 (Yuan et al., 2004).

At first, the desorption of water results in the decrease of intensity of the H_2O band and the appearance of the 3739 cm^{-1} shoulder band corresponding to the silanols (Fig. 1, *I* and *II*). With continuous desorption of water and the exposure of more and more silanols, the band becomes stronger with position progressively moving to higher wave number, and near the position of band corresponding to isolated silanol. This reflects that some strongly H-bonded silanols begin to condense to form siloxane bridges (Fig.1, scheme *III* and *IV*) while most of the isolated silanols have not condensed. This shows that for the H-bonded silanol in diatomaceous silica, the weaker the hydrogen bond is, the closer its band nears that of isolated silanol, and more difficult the occurrence of condensation is. At 1000ºC, the intensity of 3745 cm^{-1} band reached its maximum, indicating the amount of isolated silanols reached the maximum. The asymmetry of this band toward the lower wave number reflects that there are some weakly H-bonded silanols remain on the surface (Yuan et al., 2004).

2. Experimental

A natural diatomite sample from Kom Osheem deposit, Egypt was subjected to heat treatment at temperatures from 600 to 900, 1000, 1100, and 1200ºC. Soaking time was kept constant at 5 hours through all experiments. The tests were carried out in programmable furnace, with a heating rate from a room temperature to the appointed temperature of 20ºC/min. Natural diatomite means that the crude ore was subjected to size disintegration and classified to remove extraneous matter coarser than 45 micron.

Phase analysis of the treated samples was applied using X-ray diffractmeter model “pw 1010” with CuKα radiation under target voltage 40kV and current 30 mA in a scanning rate of 5º 2θ/min. Elemental chemical analysis was conducted using “Perkin-Elmer Analyst 200” atomic absorption. Thermal analysis of the sample was carried out using “Netzsch STA 409 C/CD” unit. Particle size analysis of the sample was carried out using the ‘Warman” cyclosizer. Structure skeleton of different samples have been microscopically viewed using scanning electron microscope (SEM) of the type JEM-1230, JEOL.

3. Results and discussion

3.1. Sample characterization

Phase analysis of the sample is illustrated in Fig. 2. Semi quantitative analysis of the sample showed that calcite [C], montmorillonite [M], and quartz [Q] were the main gangue minerals. They were found approximately at the ratio 4.45: 1.13:1, respectively (Table 1). Chemical analysis of the sample is shown in Table 2. From the Tables it could be concluded that diatomite mineral constituted about 80% of the sample. Particle size distribution showed that 100% of the sample was below 35 micron, whereas 94% was below 11 micron (Table 3).

Thermal analysis of the sample was depicted in Fig. 3. Figure 3 showed an endothermic pattern due to the release of diatomite absorbed water at the temperature range 100–200ºC, with a loss in sample weight reaching 0.7%. At temperature range 250- 600ºC, another endothermic reaction due to the release of the combined water of the clay mineral (300- 600°C) was recorded (Fig. 3). This endothermic reaction caused a loss in weight reaching 5.55%. An intense endothermic peak at the temperature range 600 to 750ºC due to calcite mineral break down, with a loss in weight reaching 8.95%, was depicted (Fig. 3). A loss in the sample weight reaching 1.75% was noticed at 900-1200ºC that may be attributed to the complete dehydration of diatomite structure and the formation of a new silicate material.

SEM pictures of the sample showed that the most abundant diatomite genera types were epithemia argus (long diameter 70 um and short diameter 10 um), actinocyclus ehrenbergii (diameter 14 µm), and pinnularia brevicostata ((long diameter 20 µm and short diameter 10 µm) (Fig. 4). The presence of these diatomite genera indicated the fresh water environment origin of the deposit (Moyle and Dolley, 2003). Microscopic pictures of the sample revealed the presence of intact diatomite skeletons but not clearly observed. It was noticed that the skeletons surfaces were partly masked by the impurities; meanwhile the pores were filled with minute mineral particulates and organic matter, Fig. 4.

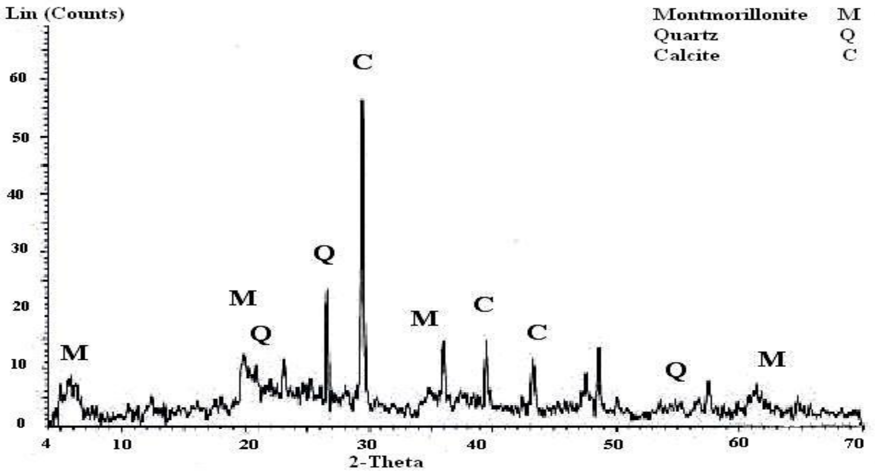

Fig. 2. XRD patterns of diatomite head sample

Table 1. Semi quantitative phase analysis of accompanied gangue minerals after XRD

Mineral	Wt.%
Quartz [Q]	15.20
Montmorillonite [M]	17.20
Calcite [C]	67.60

Table 2. Chemical analysis of the head sample

Constituent	Wt. %
SiO_2	83.60
Al_2O_3	4.24
CaO	6.17
Fe_2O_3	1.07
LOI	4.86

Table 3. Particle size distribution of the head sample

Size Fraction, um	Cum. Wt. % Retained
44	
35	
25	0.24
15	1.70
11	5.96
-11	100.00

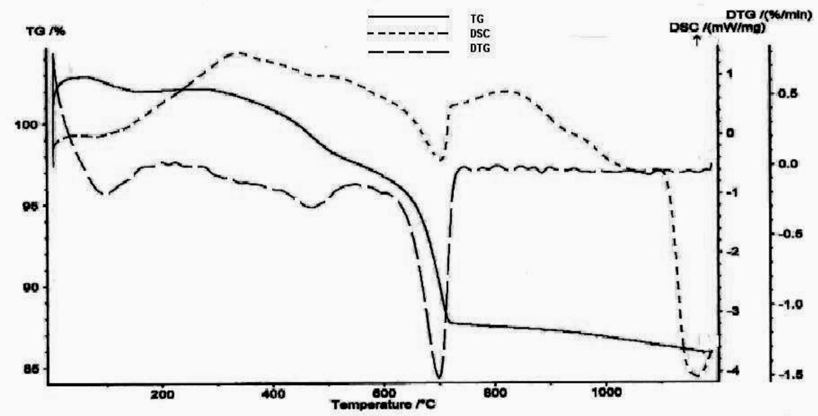

Fig. 3. Thermal analysis of diatomite sample

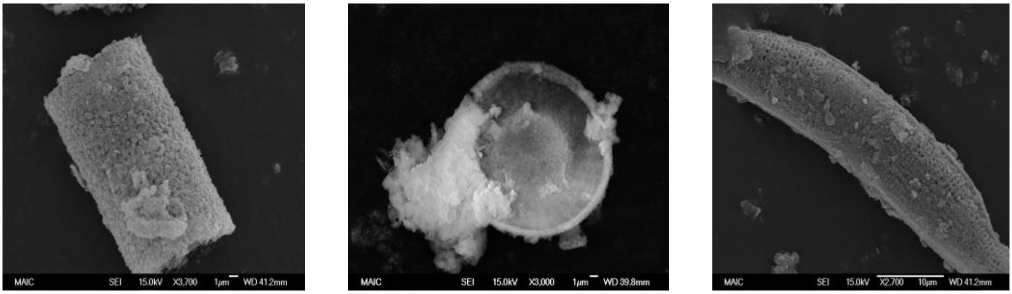

a b c

Fig. 4. Different diatomite genera, a: epithemia argus, b: actinocyclus ehrenbergii, c: pinnularia brevicostata, with complete blocked pore openings

3.2. Thermal behavior of the sample

On heating the sample at 600ºC for 5 hrs, dehydration process of diatomite surface was continued, where montmorillonite mineral was de-hydroxylated to form the amorphous meta kaolin according to the reaction (Balek and Murat, 1996):

$$Al_2O_3\,2SiO_2\,2H_2O = Al_2O_3\,2SiO_2 + 2H_2O.$$

Figure 5 illustrats the XRD pattern of the heated sample at 600ºC for 5 hrs. By comparing Figs. 2 and 5, it could be noticed that the main peak related to montmorillonite [M] at d-spacing = 15.0 (2θ=6º) disappeared due to the de-hydroxylation reaction to form metakaolin that appeared as broad noisy peaks at 2θ= 15º-30º (Balek and Murat, 1996) (Fig. 5). The fired sample at 600ºC for 5hrs showed a loss in sample weight reaching 6.39% and left behind a pink powder instead of the grey original color of the sample.

On heating the sample at 900ºC for 3 hrs wollastonite mineral was formed as a sole crystalline phase as shown in Figure 6. The mineral main peaks were shown at 2θ=30.06, 25.28, 23.20, (Fig. 6). On the other hand thermal decomposition of calcite was remarked, where complete removal of its main peaks at 2θ= 29.40, 43.14, and 39.40 was recorded (Fig. 6).

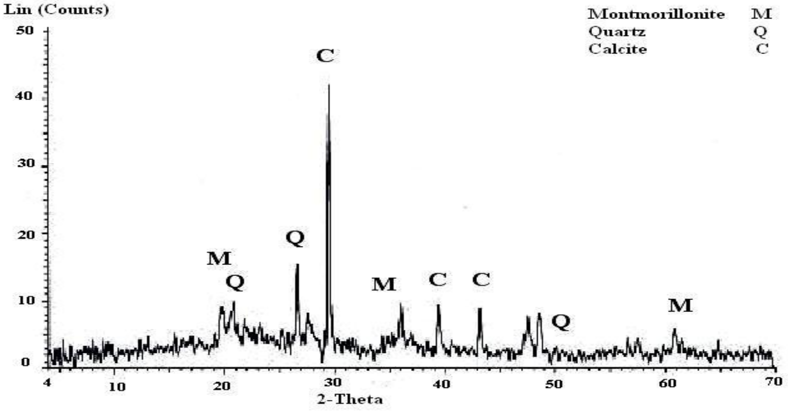

Fig. 5. XRD patterns of heated sample at 600ºC for 5hrs

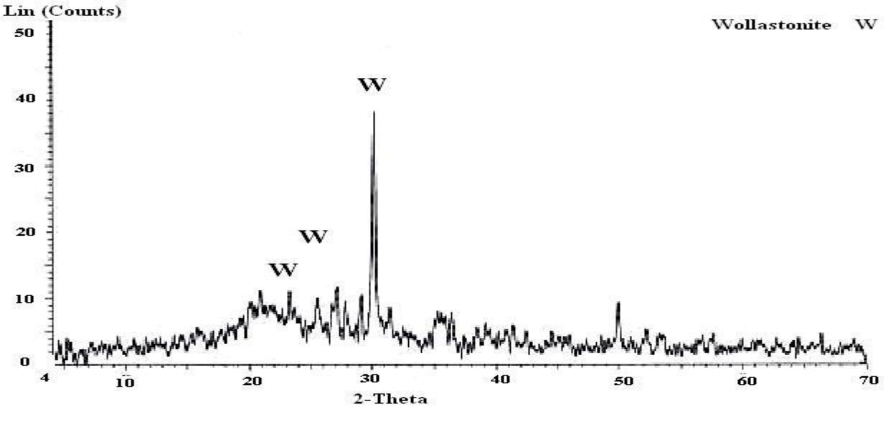

Fig. 6. XRD patterns of heated sample at 900ºC for 3hrs

The formation of wollastonite mineral [W] was explained after the reaction of the reactive lime species after calcite dissociation and reactive diatomaceous silica that was found in abundance in the heated sample (Ibrahim, 2009). A substantial increase in wollastonite peak intensity from 45% to 52.7% by increasing time of heating was remarked (Figs. 7 and 8), respectively.

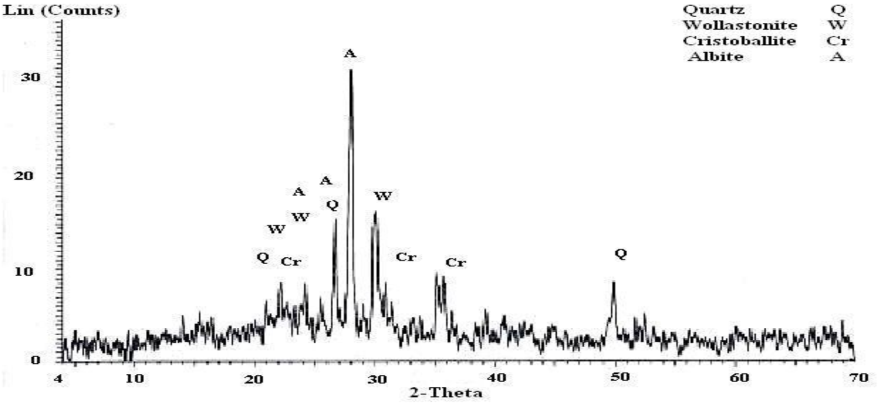

Fig. 7. XRD patterns of heated sample at 900ºC for 5hrs

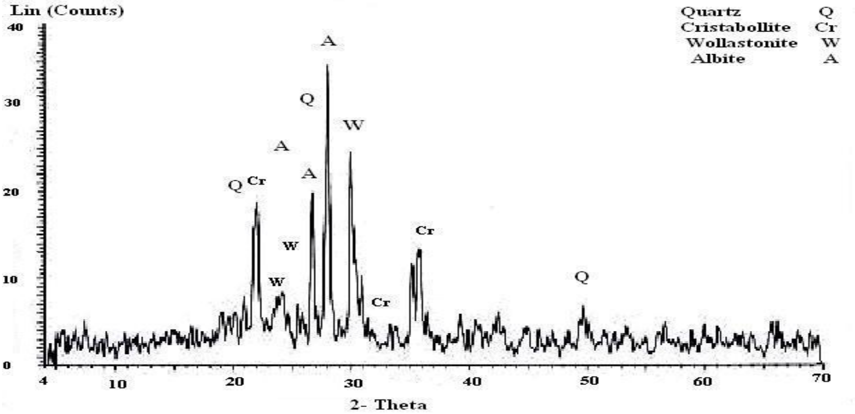

Fig. 8. XRD patterns of heated sample at 1000ºC for 5hrs

SEM pictures of the heated sample at 900ºC for 3 hrs showed that the pores openings of the diatomite porous structure became free from any blocking materials when compared to the original sample (Figs. 9 and 4), respectively. The temperature at which complete clearance of the porous structure of diatomite, i.e. calcinations temperature varied slightly from type to type, and presented an essential operation for diatomite when it was supposed to be directed to filter aid applications (Ibrahim and Selim, 2010; Ibrahim and Selim, 2011; Powers and Ibrahim, 2007).

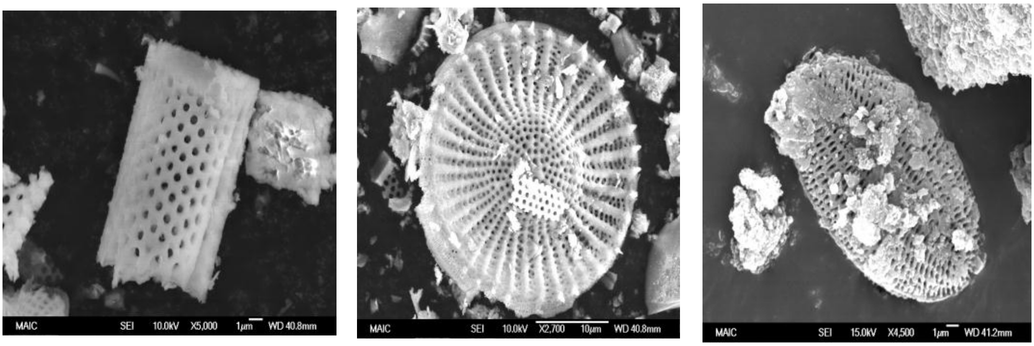

Fig. 9. SEM pictures showing the clean opened pores at 900ºC for 3 hrs

By increasing the firing soaking time to 5 hours at 900ºC, diatomite structure showed a sign of its original porous structure, but the concave and convex surfaces were almost all gone, and smoother surfaces were formed instead (Fig. 10).

On the other hand, XRD analysis of the fired sample showed a weak peak belonging to cristobalite mineral [Cr] at 2θ=21.93, 36.12, 31.46 (Fig. 8). It was suggested that the formation of cristobalite was in expense of diatomite silica, where crystalline silica formed cristobalite at 1200ºC, whereas amorphous silica like diatomite formed cristobalite at 900^{o}C (Wahl et al., 1961). Relative intensity of cristobalite peak (at $2\theta=22^{o}$) increased from 4.5% at 900^{o}C to 6.6% at 1000^{o}C (Figs. 8 and 9), respectively. The fired sample at 900ºC for 5hrs showed a loss in sample weight reaching 15.6% and left a faint brown powder behind, instead of grey original color of the sample.

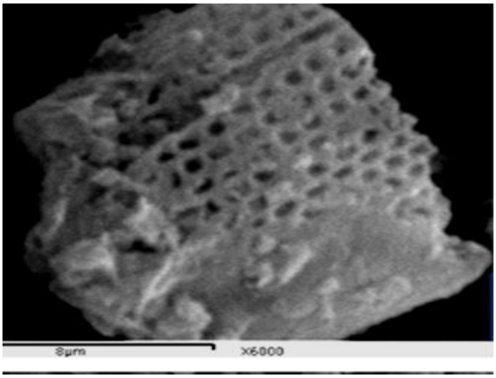

Fig. 10. Collapsing of diatomite porous structure at 900ºC for 5hrs

By increasing the firing temperature to 1000ºC for 5 hrs, complete dehydration of diatomite structure occurred which was accompanied by total collapsing and distortion of the porous structure as shown in Fig. 11. The left powder was brown in color and a pronounced loss in weight reached 19.82% was recorded.

By heating the sample at 1100ºC for 5 hrs, an olive green colored material was formed. The main XRD peaks of the product appeared at 2θ=21.93, 29.85, 35.48, and 30.88, that belonged to calcium alkali silicate mineral called diopside, (Fig. 12). Diopside is an inosilicate mineral composed of single chains of silica tetrahedra and belonging to pyroxene group. Pyroxenes have the general formula $XY(Si, Al)_2O_6$ (where X represents calcium, sodium, Fe^{+2} and magnesium and more rarely zinc, manganese and lithium and Y represents ions of smaller size, such as chromium, aluminium, iron (III), magnesium, manganese, scandium, titanium, vanadium and even iron (II). Although aluminium substitutes extensively for silicon in silicates such as feldspars and amphiboles, the substitution occurs only to a limited extent in most pyroxenes (Morimoto et al., 1989). The formed product showed loss on sample weight that reached 23.08% with a hard vitreous texture.

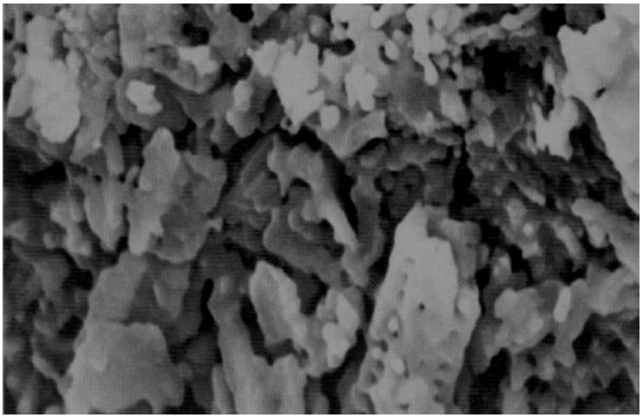

Fig. 11. Complete destroying of diatomite porous structure at 1000ºC

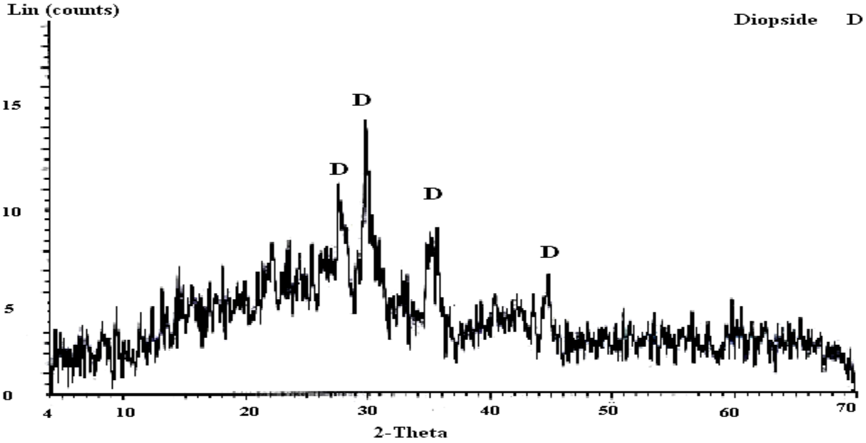

Fig. 12. XRD patterns of heated sample at 1100ºC for 5hrs

Figure 13 illustrates the XRD pattern of the sample after heating at 1200ºC for 5 hrs. The formed sample was a nano-metric vitreous glassy material (Fig. 14) that showed remarkable reduction in volume compared to the sample heated at 900ºC for 5 hrs (Fig. 15).

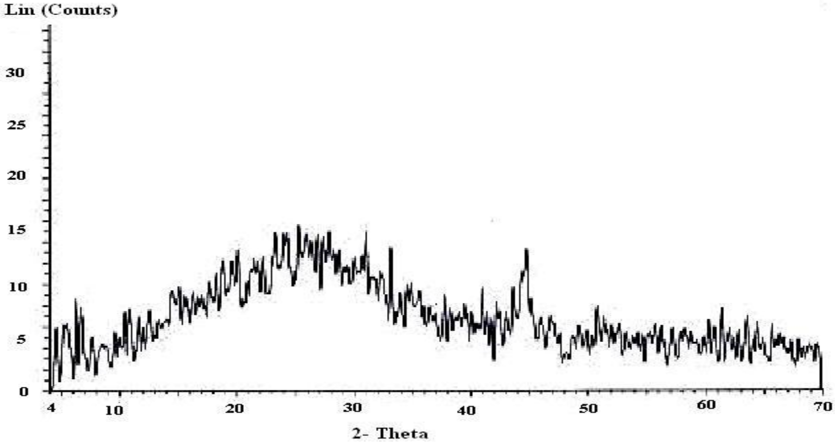

Fig. 13. XRD patterns of heated sample at 1200ºC for 5hrs

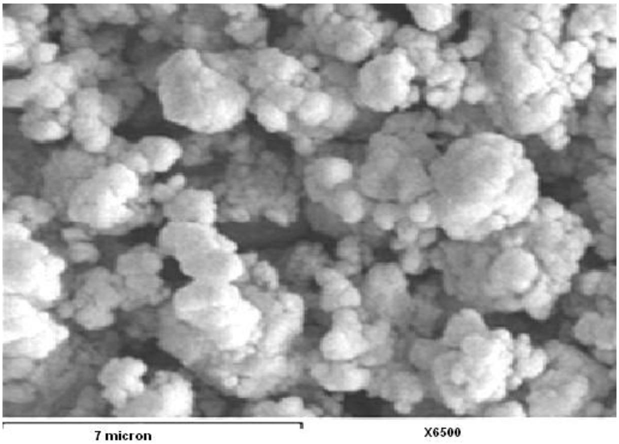

Fig. 14. SEM picture of the new material formed at 1200ºC

4. Conclusions

Natural diatomite sample from Kom Osheem Localiy, El-Fayoum Depression, Egypt was subjected to heat treatment. The main accompanied minerals were calcite, montmorillonite and quartz. The sample was soaked for 5 hrs at temperatures of 600, 900, 1000, 1100, and 1200ºC. Characterization of the heated samples was followed up by using XRD and SEM techniques and other physical characterization like the detection of sample color, texture, and weight loss. Results showed that by heating the sample at different temperatures for 5 hrs, various transformation reactions from mineral to another was occurred. On the other hand, results showed that at 900ºC for 3 hrs the diatomite porous structure was completely calcined and improved. Partial collapsing of this porous structure started by heating the sample at 900ºC for 5 hrs, where complete destruction was remarked at 1100ºC with the formation of a nano-metric garnet like material at 1200ºC.

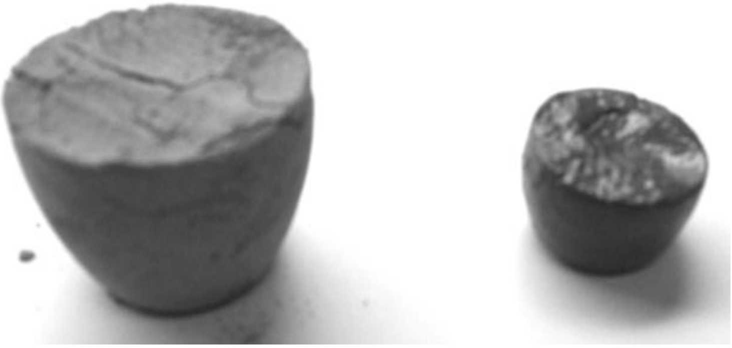

Fig. 15. Change in colour and volume of heated samples (A) at 900ºC and (B) at 1200ºC

References

BALEK V., MURAT M., 1996, *The emanation thermal analysis of kaolinite clay minerals*, Thermochim. Acta, 282–283, 385–397.

BRONNIMANN C.E., ZEIGLER R.C., MACIEL G.E., 1988, *Proton NMR study of dehydration of the silica gel surface*, J. Am. Chem. Soc., 110, 2023–2026..

EK S., ROOT A., PEUSSA M., NIINISTO L., 2001, *Determination of the hydroxyl group content in silica by the thermogravimetry and a comparison with HMAS NMR results*, Thermochim. Acta, 379, 201–212.

ERDOGAN B., DEMIRCI S., AKAY Y., 1996, *Treatment of sugar beet juice with bentonite, sepiolite, diatomite, and quartamin to remove color and turbidity*, Appl. Clay Sci. 11, 55–67.

IBRAHIM S.S., 2007, *Preparation of wollastonite mineral from Egyptian crude minerals*, Egyptian Academy of Scientific Research and Technology.

IBRAHIM S.S., SELIM A.Q., 2011, *Evaluation of Egyptian diatomite for filter aid applications*, Physicochem. Probl. Miner. Process., 47, 113–122.

IBRAHIM S.S., SELIM A.Q., 2010, *Producing a micro-porous diatomite by a simple classification-calcination process*, The Journal of Ore Dressing 2(23), 25–33.

JONES J.B., SEGNIT, E.R., 1971, *The nature of opal 1. nomenclature and constituents phases*, J. Geol. Soc., Aust. 18, 57–68.

LI X., BIAN C., CHEN W., HE J., WANG Z, XU N, XUE G, 2003, *Polyaniline on surface modification of diatomite: A novel way to obtain conducting diatomite fillers*, Appl. Surf. Sci. 207, 378–383.

MORIMOTO N., FABRIES J., FERGUSON A.K., GINZBURG I.V., ROSS M., SEIFEIT F.A., ZUSSMAN J., 1989, *Nomenclature of pyroxenes*, Canadian Mineralogist 27, 143–156.

MOYLE P.R., DOLLEY T.P., 2003, *A comparison of marine and continental-lacustrine diatomite deposits*, Industrial-Minerals Research.

POWERS K., IBRAHIM S.S., 2009, *Preparation of different diatomite concentrates for various industrial applications*, International Science and Engineering, NSF, USA.

STERRENBURG F., GORDON RJ., TIFFANY M.A., NAGY S.S., 2007, *Algae and cyan-bacteria in extreme environments*, Springer, 141–172.

TAKEI T., KATO K., MEGURO A., CHIKAZAWA M., 1999, *Infrared Spectra of Geminal and Novel Triple Hydroxyl Groups on Silica Surfaces,* Colloids and Surfaces, A: Physicochemical and Engineering Aspects, Vol. 150, No. 1, 77–84.

VASCONCELOS P.V., LABRINCHA J.A., FERREIRA J.M.F., 2000, *Permeability of diatomite layers processed by different colloidal techniques*, J. Eur. Ceram. Soc. 20, 201–207.

WAHL F.M., GRIM R.E., GRAF R.B., 1961, *Phase Transformations in Silica as Examined by Continuous X-ray Diffraction*, The American Mineralogist, 46, 1064–1076.

YUAN P., WU D.Q., HE H.P., LIN Z.Y., 2004, *The hydroxyl species and acid sites on diatomite surface: A combined IR and Raman study*, Applied Surface Science, 227, 30–39.